

# Sunyaev Zel'dovich high resolution view of filamentary structures between galaxy clusters pairs

Federico Radiconi

supervisor: Elia Battistelli



SAPIENZA  
UNIVERSITÀ DI ROMA

# 'Missing Baryons'

About half of the baryonic matter in the local Universe is not directly observable.

These 'missing baryons' could be in plasma outside galaxy clusters ([Fukugita et al. 1998](#)), a hypothesis confirmed by hydrodynamical simulations ([Cen & Ostriker 1999](#)).

~30% of baryons in the local Universe must reside in diffuse low density and hot ( $10^5 - 10^7$  K) gas in the outskirts of galaxy clusters and along filaments connecting them into the so called cosmic web ([Tuominen et al 2021](#)).

Observing these 'missing baryons is challenging':

- Low gas density means faint X-ray emission ( $L_x \sim n^2$ )
- Low relativistic electrons number and weak magnetic fields makes radio observations very demanding

One way to detect these baryons is the Sunyaev-Zeldovich (SZ) effect: inverse Compton scattering of CMB photons with hot electrons in the intracluster medium. Thermal SZ amplitude is proportional to the Compton  $y$ -parameter:

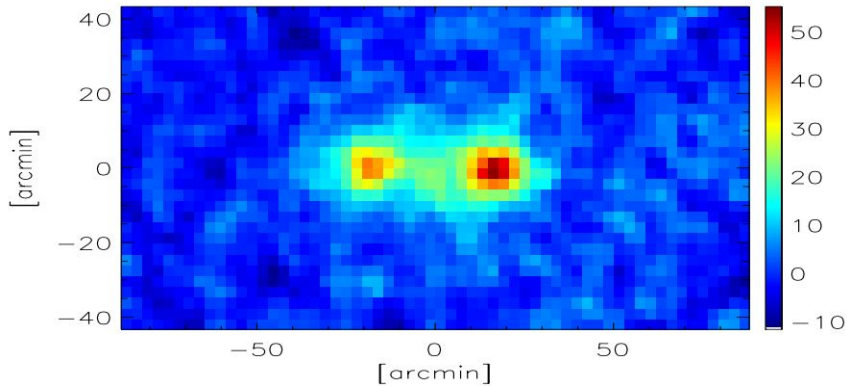
$$y = \frac{\sigma_T}{m_e c^2} \int P_e(r) dr = \frac{\sigma_T}{m_e c^2} \int n_e(r) k_B T_e(r) dr$$

Low  $z$  cluster pairs can be perfect laboratories to observe these 'missing baryons' as filaments connecting them.

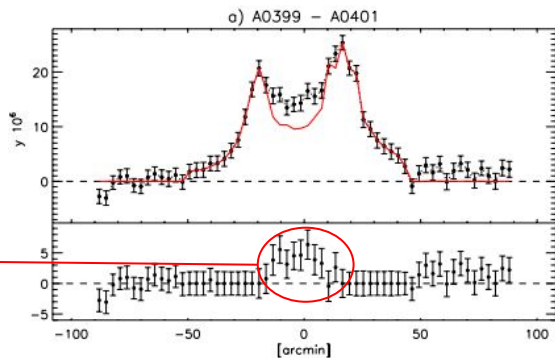
# Abel 399-Abell 401 system ( $z \sim 0.07$ )

[Planck Collaboration et al. \(2013\)](#)

a) tSZ for A0399-A0401

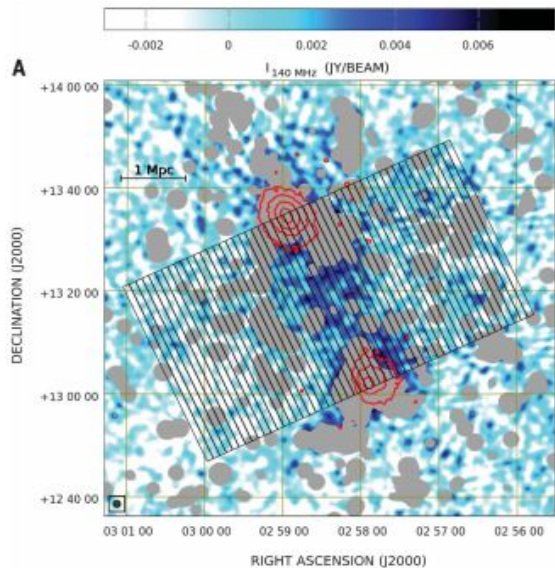


Planck y-map  
7.18' resolution



Excess after clusters  
removal  
(only  $\sim 3$  Planck beams)

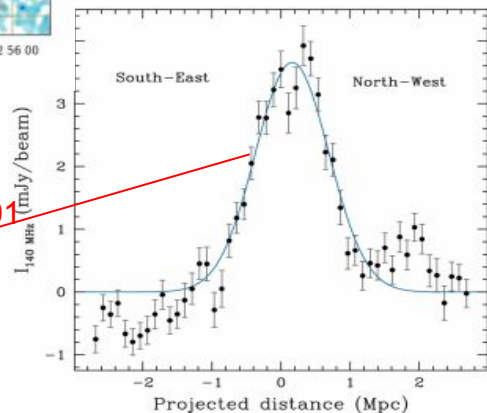
[Govoni et al. \(2019\)](#)



LOFAR 140 MHz  
80'' resolution

Radio 'ridge' between A399-401

$B < 1 \mu\text{G}$



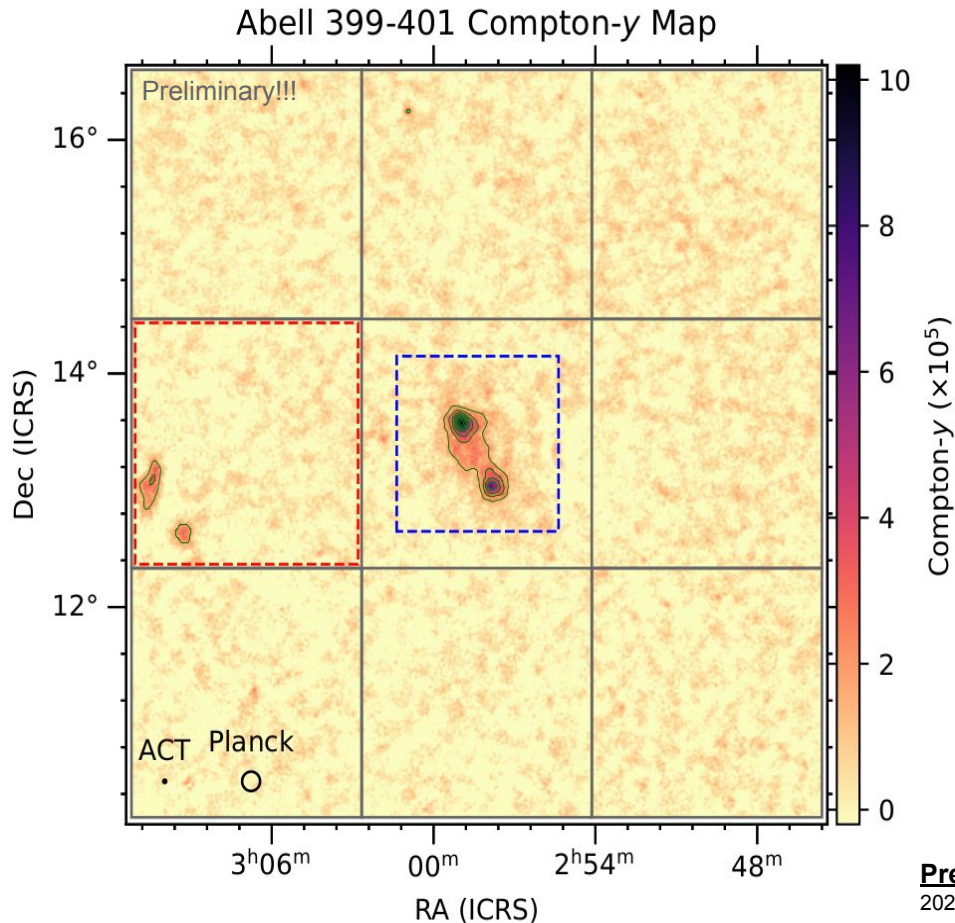
# The Atacama Cosmology Telescope

- 6 m CMB telescope located at 5190 m altitude on the Chajnator plateau in the Atacama desert
- Observing since 2008
- High resolution (1-2 arcmin) temperature and polarization at: 98, 150 and 220 GHz
- 2 bands at 30 and 40 GHz added in 2020
- Together with SPT are the only high-resolution ( $\sim$ arcmin) CMB survey telescopes



Image credit: Debra Kellner

# A399-401 ACT Compton- $\gamma$ map



- Using the 98, 150 and 220 GHz ACT + Planck maps ([Madhavacheril et al. 2020](#))
- Main difference with respect to ACT DR5 ([Naess et al 2020](#)) is the inclusion of 2019 ACT data
- 1.65' angular resolution
- Zero-lag noise:  $\sigma = 5.9 \times 10^{-6}$  y/pixels
- Green contours levels are 3, 5, 7, 9, 11, 13, and  $15\sigma$
- ❖ outer green boxes = Used to extract the Covariance Matrix ( $M$ )
- ❖ Dashed Red = Dust contaminated region, excluded to estimate  $M$

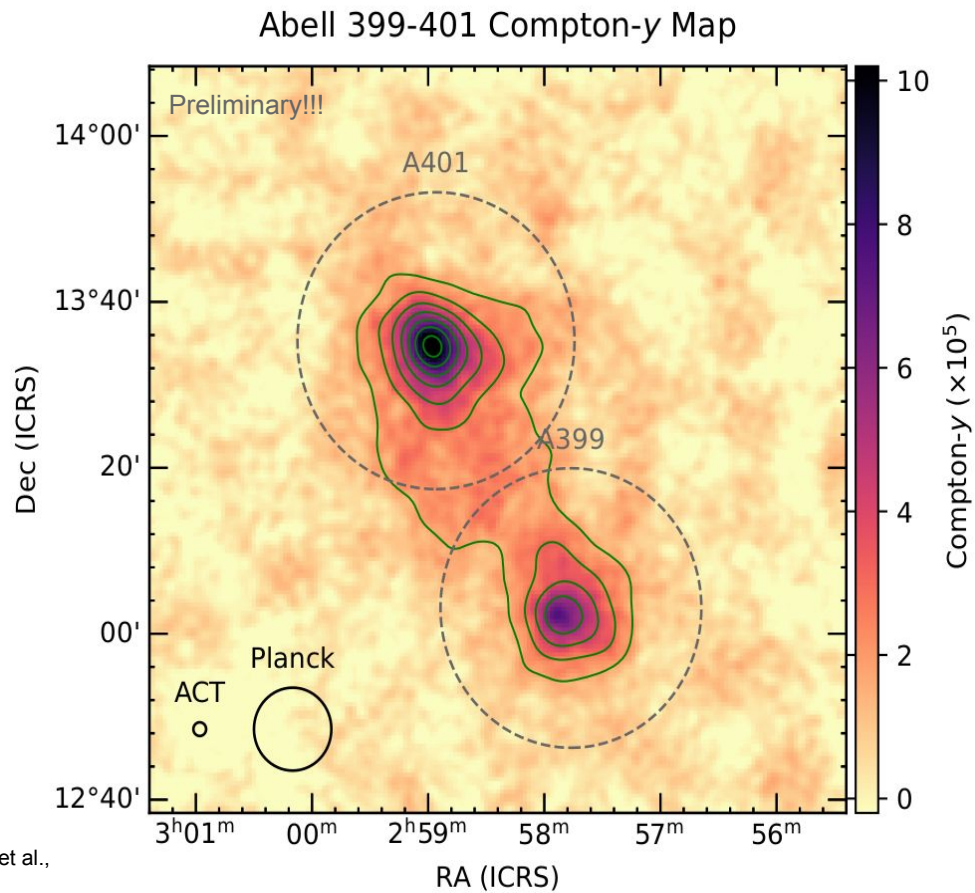


# A399-401 ACT Compton-y map

ACT map zoom in (dashed blue region).

Contours levels are 3, 5, 7, 9, 11, 13, and 15 $\sigma$

Dashed circles corresponding to their measured  $R_{500}$



# Fitted Models

We fitted four models with a MCMC algorithm (*emcee*, [Foreman-Mackey et al. 2013](#)):

- 1) 2 Elliptical  $\beta$ -profiles for A399 and A401
- 2) 3 Elliptical  $\beta$ -profiles for A399, A401 and the bridge region
- 3) 2 azimuthally-symmetric (Circular)  $\beta$ -profiles for A399 and A401 + mesa model for the bridge
- 4) 2 Elliptical  $\beta$ -profiles for A399 and A401 + mesa model for the bridge

Circular  $\beta$ -profiles ([Cavaliere & Fusco-Femiano 1978](#))

$$P(r) = k_B T_e \frac{n_0}{\left[1 + \left(\frac{r}{r_c}\right)^2\right]^{\frac{3}{2}\beta}}$$

$\beta$ -profiles asphericity ([Hughes & Birkinshaw 1998](#))

$$\frac{r}{r_c} \rightarrow \frac{\sqrt{x^2 + (y/R)^2}}{r_c}$$

Mesa model

*Ad hoc* model to capture the apparent flatness of the inter-cluster excess (see previous slides) with minimal assumptions about its precise shape

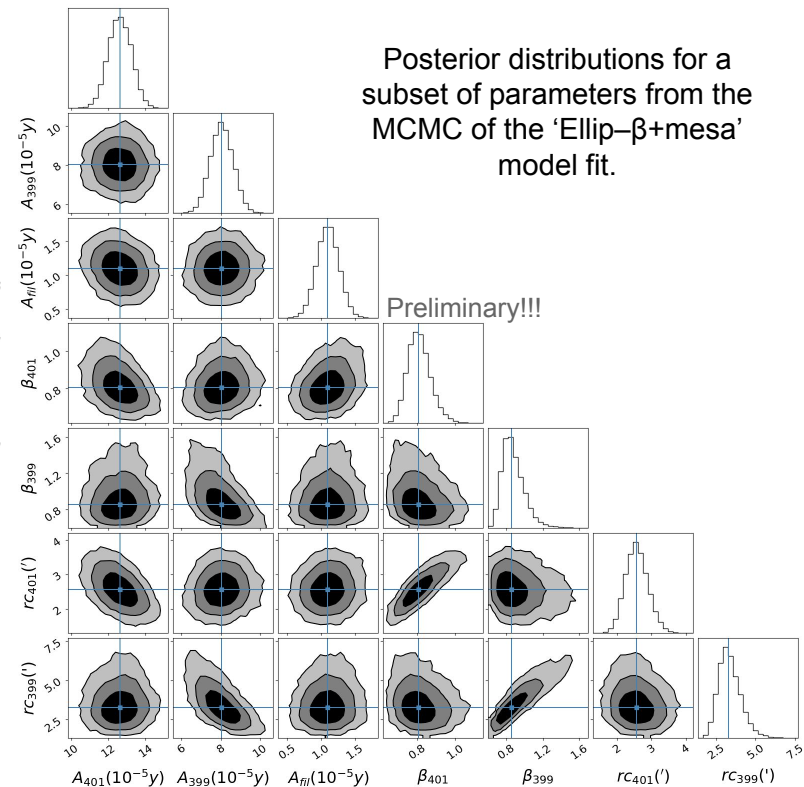
$$g(l, w) = \frac{A_{\text{fil}}}{1 + \left(\frac{l}{l_0}\right)^8 + \left(\frac{w}{w_0}\right)^8}$$

# Fit Results

Model	A399							Preliminary!!!
	$A$ ( $10^{-5}y$ )	$\alpha$ ( $^\circ$ )	$\delta$ ( $^\circ$ )	$\beta$	$r_c$ ( $'$ )	$\theta$ ( $^\circ$ )	$R$	
Ellip- $\beta$ , no bridge	$8.2^{+0.6}_{-0.6}$	$44.474 \pm 0.003$	$13.030 \pm 0.003$	$0.74^{+0.08}_{-0.07}$	$2.7^{+0.6}_{-0.5}$	$-53^{+18}_{-18}$	$0.87^{+0.07}_{-0.07}$	
3 $\times$ Ellip- $\beta$	$7.9^{+0.6}_{-0.6}$	$44.473 \pm 0.004$	$13.030 \pm 0.003$	$0.84^{+0.13}_{-0.09}$	$3.1^{+0.8}_{-0.6}$	$-47^{+27}_{-26}$	$0.92^{+0.05}_{-0.07}$	
Circ- $\beta$ +mesa	$8.2^{+0.8}_{-0.6}$	$44.473 \pm 0.004$	$13.030 \pm 0.003$	$0.80^{+0.10}_{-0.08}$	$2.9^{+0.6}_{-0.5}$	N/A	1.0	
Ellip- $\beta$ +mesa	$8.1^{+0.6}_{-0.6}$	$44.473 \pm 0.004$	$13.030 \pm 0.003$	$0.81^{+0.11}_{-0.08}$	$3.0^{+0.7}_{-0.6}$	$-47^{+27}_{-26}$	$0.93^{+0.05}_{-0.07}$	

Model	A401						
	$A$ ( $10^{-5}y$ )	$\alpha$ ( $^\circ$ )	$\delta$ ( $^\circ$ )	$\beta$	$r_c$ ( $'$ )	$\theta$ ( $^\circ$ )	$R$
Ellip- $\beta$ , no bridge	$13.2^{+0.6}_{-0.6}$	$44.750 \pm 0.002$	$13.569 \pm 0.002$	$0.73^{+0.04}_{-0.04}$	$2.4^{+0.3}_{-0.3}$	$-61^{+6}_{-6}$	$0.77^{+0.05}_{-0.05}$
3 $\times$ Ellip- $\beta$	$11.8^{+0.8}_{-1.0}$	$44.750 \pm 0.002$	$13.572 \pm 0.002$	$0.93^{+0.18}_{-0.10}$	$2.9^{+0.5}_{-0.4}$	$-56^{+10}_{-9}$	$0.83^{+0.06}_{-0.05}$
Circ- $\beta$ +mesa	$12.7^{+0.6}_{-0.6}$	$44.750 \pm 0.002$	$13.572 \pm 0.002$	$0.83^{+0.06}_{-0.05}$	$2.4^{+0.3}_{-0.3}$	N/A	1.0
Ellip- $\beta$ +mesa	$12.6^{+0.6}_{-0.6}$	$44.751 \pm 0.002$	$13.572 \pm 0.002$	$0.82^{+0.07}_{-0.06}$	$2.6^{+0.4}_{-0.3}$	$-57^{+9}_{-8}$	$0.82^{+0.06}_{-0.05}$

Model	Bridge							
	$A_{\text{fl}}$ ( $10^{-5}y$ )	$\alpha$ ( $^\circ$ )	$\delta$ ( $^\circ$ )	$l_0$ ( $'$ )	$w_0$ ( $'$ )	$r_c$ ( $'$ )	$\theta$ ( $^\circ$ )	$R$
Ellip- $\beta$ , no bridge	—	—	—	—	—	—	—	—
3 $\times$ Ellip- $\beta$	$2.01^{+0.52}_{-0.41}$	$44.69^{+0.03}_{-0.03}$	$13.40^{+0.06}_{-0.05}$	—	—	$16.0^{+1.7}_{-2.4}$	fix	$0.80^{+0.13}_{-0.12}$
Circ- $\beta$ +mesa	$1.20^{+0.17}_{-0.17}$	$44.67^{+0.01}_{-0.01}$	$13.35^{+0.02}_{-0.03}$	$11.7^{+1.4}_{-1.2}$	$10.6^{+1.0}_{-0.9}$	—	fix	—
Ellip- $\beta$ +mesa	$1.10^{+0.17}_{-0.18}$	$44.68^{+0.02}_{-0.02}$	$13.37^{+0.02}_{-0.03}$	$12.3^{+1.7}_{-1.4}$	$10.8^{+1.1}_{-1.0}$	—	fix	—

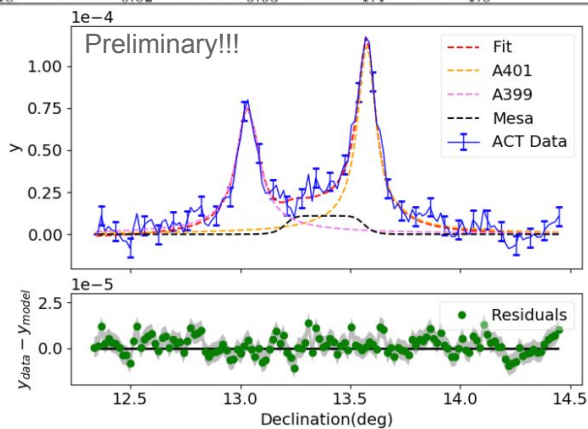


Posterior distributions for a subset of parameters from the MCMC of the 'Ellip- $\beta$ +mesa' model fit.

Preliminary!!!

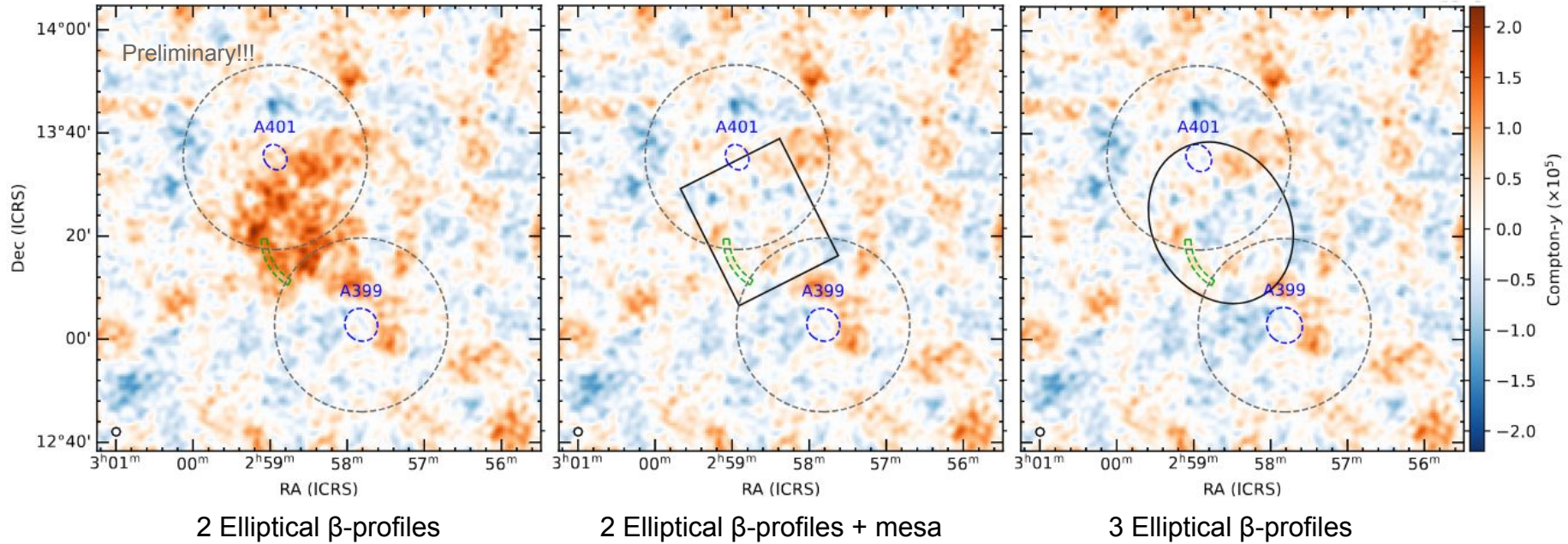
**Preliminary!!!** Hincks A.D., Radiconi F., Romero C., Madhavacheril M.S., Mroczkowski T., et al., 2021 (in prep.)

1D profile of the best fit 'Ellip- $\beta$ +mesa' model.





# Residuals



Green dashed region indicate the shock region identified in [Akamatsu et al. \(2017\)](#).

# Models comparison

Data	Model	$P$	Likelihood Ratio		AIC $w_i$
			$W$	$\sigma$	
<i>ACT+Planck</i>	Ellip- $\beta$ , no bridge	17	—	—	$4.3 \times 10^{-8}$
	3 $\times$ Ellip- $\beta$	22	33.2	4.6	0.0047
	Circ- $\beta$ +mesa	18	—	—	0.23
	Ellip- $\beta$ +mesa	22	43.4	5.5	0.77
<i>Planck</i> only	Ellip- $\beta$ , no bridge	17	—	—	0.0012
	Ellip- $\beta$ +mesa	22	23.5	3.6	0.999

- $P$  = Free Parameters
- Likelihood ratio  $W = 2 \log \frac{\max \mathcal{L}_2}{\max \mathcal{L}_1}$  (only valid if Model 1 is an extension of Model 2)
- AIC = [Akaike Information Criterion](#),  $w_i$  is the relative probability

# Derived Quantities

From 2 Elliptical  $\beta$ -profiles + mesa best fit model we extracted:

- Mesa Compton integrated:  $Y_{\text{mesa}} = (4.9 \pm 1.0) \times 10^{-5} \text{Mpc}^2$
- Mesa mass:  $M_{\text{mesa}} = (3.3 \pm 0.7) \times 10^{14} M_{\odot}$  (gas + dark matter)
- Clusters masses:  
 $M_{200, A399} = (18.1 \pm 2.2) \times 10^{14} M_{\odot}$  &  $M_{200, A401} = (21.3 \pm 2.7) \times 10^{14} M_{\odot}$

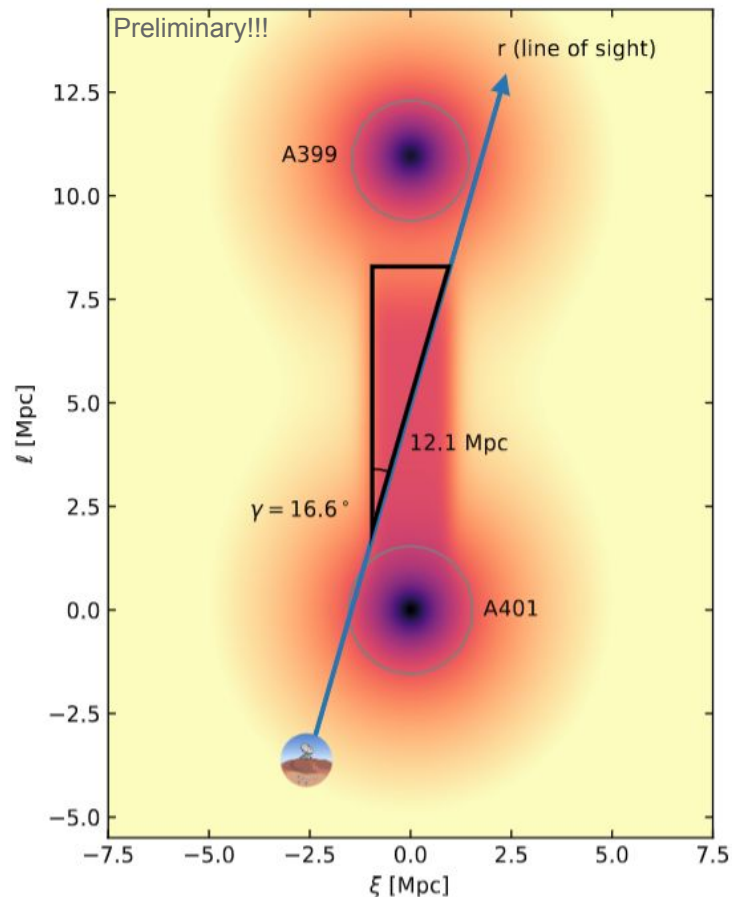
$$M_{\text{mesa}} / (M_{200, A399} + M_{200, A401}) \approx 8\%$$

- Mesa sizes (on the sky):  $l_{\text{fil}} \times w_{\text{fil}} = 2.2 \times 1.9 \text{Mpc}^2$
- $y$  at the Mesa center (Mesa + clusters halos):  $y_{\text{tot}} = (2.8 \pm 0.3) \times 10^{-5}$
- Assuming  $kT_{\text{fil}} = 6.5 \text{keV}$  ( [Akamatsu et al. 2017](#) ) and  $y_{\text{tot}} = (8.0 \pm 1.0) \times (r_{\text{fil}}/\text{Mpc})^{0.5} \times 10^{-6}$

$$\text{---> } r_{\text{fil}} = (12.1 \pm 3.9) \text{Mpc} \quad \& \quad n_e = (0.88 \pm 0.24) \times 10^{-4} \text{cm}^{-3}$$

**Thickness along the l.o.s.  $r_{\text{fil}} \gg l_{\text{fil}} \ \& \ w_{\text{fil}}$**

# Toy Model



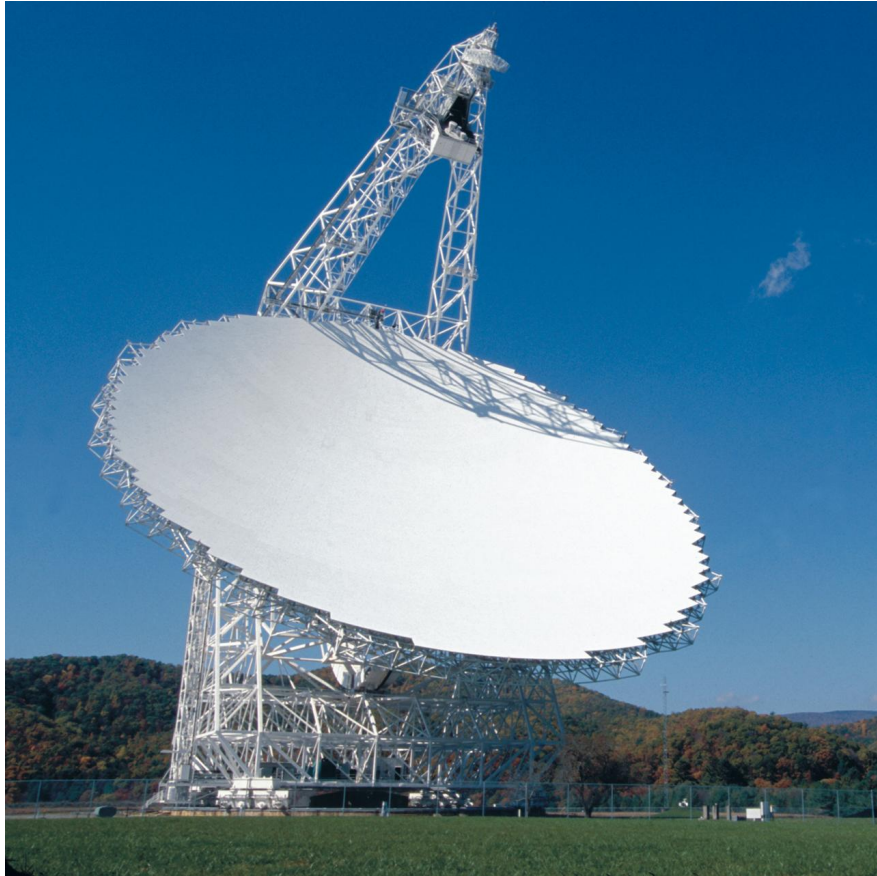
- Assuming a symmetric filament along the line connecting A399-401, so true thickness =  $w_{\text{fil}}$
- Angle between l.o.s. and A399-401 axis (Mesa+cluster halos):  
 $\gamma \propto \arcsin(w_{\text{fil}} / r_{\text{fil}}) = \mathbf{16.6^{+5.5}_{-3.8} \text{ deg}}$
- A399-401 separation on the sky  $d_p = 3.2 \text{ Mpc}$   
 ---> total separation  $\mathbf{d_T = 12.1^{+3.4}_{-2.8} \text{ Mpc}}$

Despite the highly idealized model we stress that combining  $y$  in the bridge and X-ray we find that A399-401 system has a significant component along the line of sight. Previous studies implicitly assume that the system lies almost entirely on the plane of the sky!!!!

Grey circles indicate:

$$R_{500, \text{A399}} = (1.45 \pm 0.21) \text{ Mpc} \ \& \ R_{500, \text{A401}} = (1.53 \pm 0.19) \text{ Mpc} < \mathbf{d_T}$$

# Mustang-2 @ Green Bank Telescope (GBT)



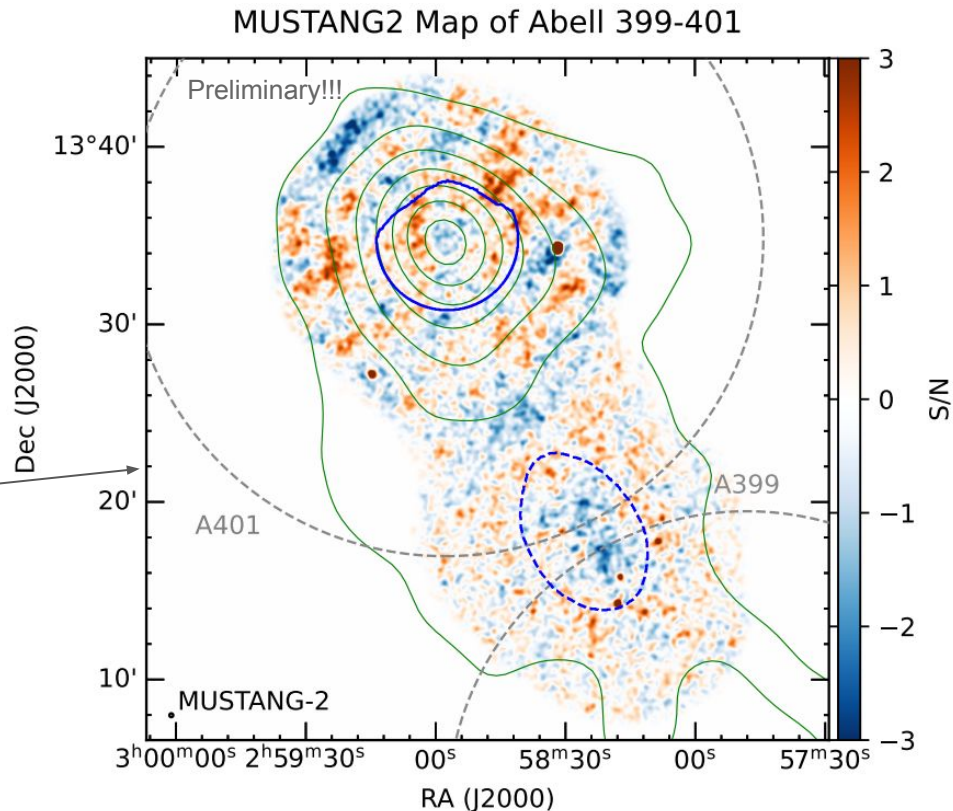
Credit: NRAO/AUI/NSF

- GBT primary mirror diameter: **100 m**
- GBT Frequency coverage: 100 MHz-100 GHz
- Protected by a 13000 km<sup>2</sup> Radio Quiet Zone
- GBT observational capabilities: Spectroscopy, Continuum, Pulsar, VLBI
- Mustang-2 (M2) is a 223-feedhorn bolometer camera operating @ 90GHz
- M2 Angular resolution: ~ 9''
- M2 FOV: ~ 4.25'
- Zenith opacity @ 90 GHz ~ 0.1; PWV  $\lesssim$  10 mm (<https://www.gb.nrao.edu/mustang/wx.shtml>)



# Mustang-2 Data

- 66 hours of observing time. 44 h on source (P.I. E. Battistelli)
- We observed A401 and the intracluster(Mesa) region
- A399 has not been observed!!!!
- 'Preliminary' analysis using MIDAS ([Romero et al. 2020](#)) pipeline
- SNR map contains the scales from  $12.7'' < \theta < 180''$
- No imprints for large scale structures!!!

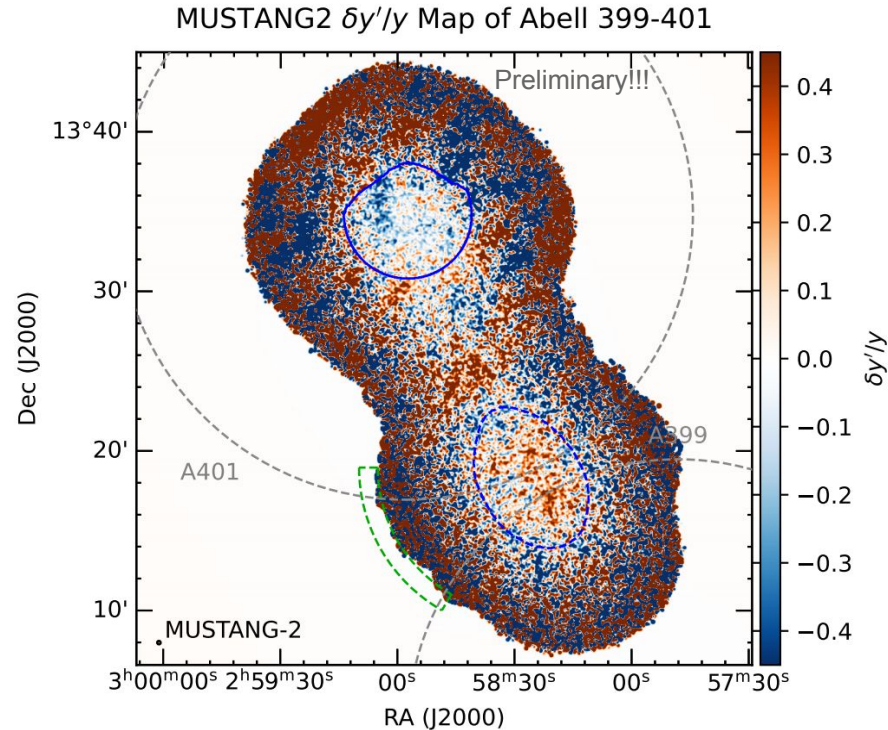


# Fluctuations

- We used the M2 map to study small-scale features in the intracluster (Mesa center) and A401 regions (blue lines).
- Map of  $\delta y'/y$  using M2 map and ACT 2-Elliptical  $\beta$ -profiles + Mesa best fit model:
  - $\delta y' = y' - \underline{y}'$
  - $y' =$  M2 Midas map
  - $\underline{y}' =$  model filtered through the MUSTANG-2 pipeline
  - $y =$  best-fit 'Ellip- $\beta$ +Mesa' model
- Intracluster region (noise < 2.9  $\mu\text{K-arcmin}$ ) =  $0.078 \pm 0.015$
- A401 (noise < 13.5  $\mu\text{K-arcmin}$ ) =  $0.052 \pm 0.022$

Low level fluctuations in both regions!!

- A401 level suggest no major merger activity, but would allow for minor ongoing mergers
- Intracluster region ---> there are not strong theoretical expectations. The geometry of the system may erase fluctuations when projected on the sky??



# Conclusions

- Low  $z$  cluster pairs are the perfect science case to study the SZ signal from the hot gas in filamentary structures
- High angular resolution ( $\sim$  arcmin) data play key role in studying systems properties
- By including ACT data, we increase the filament detection with respect to Planck only data
- A399-401 system has a significant component along the line of sight

## Next

- Hincks A.D. et al., 2021 (in prep.) will be soon be publicly available and submitted.
- Shocks search adding new deep observations of A399-401 with ACT currently unprocessed (6x better resolution than Planck at same  $\nu$ ) and combining ACT with Mustang-2 data ( $\sim 10''$  resolution, 10-15 x better resolution than ACT at 98 and 150 GHz)
- New ACT data of A399-401 + other cluster pairs stack ---> possible study of kSZ effect